Arab J Sci Eng (2014) 39:6055–6067
DOI 10.1007/s13369-014-1238-9

RESEARCH ARTICLE - CIVIL ENGINEERING

Experimental Study on the Pore Water Pressure Generation Characteristics of Saturated Silty Sands

Mostefa Belkhatir · Tom Schanz · Ahmed Arab · Noureddine Della

Received: 26 October 2011 / Accepted: 30 September 2013 / Published online: 2 July 2014

Abstract The excess pore water pressure produced during earthquake shaking causes liquefaction and influences significantly the shear strength, deformation and settlement characteristics of granular soil deposits. Therefore, the stability of the structures constructed from these deposits or founded on them is adversely affected. The mechanisms of pore pressure generation and, in turn, liquefaction resistance of granular soils are still not fully clear and require further research. For the purpose of clarifying and evaluating pore pressure buildup characteristics of sandy soils, a series of undrained monotonic triaxial tests were carried out on different reconstituted samples of sand–silt mixture at various intergranular void ratios. The soil samples were tested under a constant confining pressure ($\sigma_3' = 100\,\text{kPa}$) and at three relative densities ($D_r = 20, 53$ and $91\,\%$). The results obtained from this study reveal that the fraction of low plastic fines plays an important role in the generation of excess pore water pressure in samples of the Chlef sand–silt mixtures. It was found that excess pore water pressure can be correlated with the undrained shear strength at the peak for the range of fines' content under consideration. The gross and intergranular void ratios appear as pertinent parameters to represent the pore water pressure response of the sand–silt mixtures for a given fines' content.

Keywords Liquefaction resistance · Silty sand · Pore pressure · Fines' content · Mixtures · Gross void ratio

الخلاصة

يسبب فائض ضغط المياه المسامي الذي ينتج في أثناء الاهتزاز الزلزالي تميعيا، ويؤثر بشكل كبير في قوة القص وخصائص التشوه والتسوية لترسبات التربة الحبيبية. وبالتالي، فإن استقرار الهياكل التي شيدت من هذه الترسبات أو التي تأسست عليها يتأثر سلبا. وآليات توليد الضغط المسامي الذي يؤدي إلى مقاومة تمييع التربة الحبيبية لا تزال غير واضحة تماما ، وتحتاج إلى مزيد من البحث. ولغرض توضيح وتقييم خصائص تراكم ضغط مسام التربة الرملية نفذت سلسلة من الاختبارات ثلاثية المحور الرتيبة وغير المستنزفة على عينات مختلفة معاد تشكيلها من خليط الرمال والطمي عند نسب مختلفة من الفراغات الحبيبيـة الداخليـة. وقد تم اختبار عينات التربة تحت ضغط حصر ثابت (σ_3' = 100 كيلو باسكال) وثلاث كثافات نسبية (الكثافة النسبية = 20 ، 53 ٪ و 91 ٪). وتكشف النتائج التي تم الحصول عليها من هذه الدراسة أن الجزء من دقائق البلاستيك المنخفضة يلعب دورا هاما في توليد ضغط المياه المسامي الزائد في عينات من شلف مخاليط الرمال والطمي. وتبين أن ضغط المياه المسامي الزائد يمكن ربطه بقوة القص غير المستنزفة عند قمة مجموعة من محتويات الدقائق الناعمة المنظور فيها. وتُظهرُ نسب الفراغات الحبيبية الداخلية والإجمالية معلمات ذات صلة لتمثيل استجابة ضغط المياه المسامي من خلائط الرمال والطمي لمحتوى الدقائق الناعمة المعطاة.

List of symbols

G_f	Specific gravity of fines
G	Specific gravity of sand–silt mixture
F_C	Fines' content
γ_d	Post-consolidation dry unit weight
D_{10}	Effective grain size
D_{50}	Mean grain size
C_u	Coefficient of uniformity
C_c	Coefficient of curvature
e_{max}	Maximum gross void ratio
e_{min}	Minimum gross void ratio
I_p	Plasticity index

M. Belkhatir (✉) · A. Arab · N. Della
Laboratory of Materials Sciences and Environment,
University of Chlef, Chlef, Algeria
e-mail: abelkhatir@yahoo.com

T. Schanz
Laboratory of Foundation Engineering, Soil and Rock Mechanics,
Bochum Ruhr University, Bochum, Germany

D_r	Post-consolidation relative density
e	Post-consolidation gross void ratio
e_s	Intergranular void ratio at the end of consolidation
q_{peak}	Undrained monotonic peak shear strength
Δu	Excess pore water pressure
α	Slope
R^2	Coefficient of determination

1 Introduction

An earthquake of magnitude of 7.3 (wave magnitude of 7.3) occurred on October 10, 1980, at 13:25:23.7 local time (12:25:23.7 GMT). The epicenter of the earthquake main shock was located 12 km in the east region of Chlef City (210 km west of Algiers) at latitude of 36.143°N and a longitude of 1.413°E with a focal depth of about 10 km. The approximate duration of the quake was between 35 and 40 s. The event, commonly referred to as the El Asnam Earthquake, was among the most disastrous earthquakes that have affected the northern region of Algeria. The earthquake devastated the city of El Asnam, population estimated at 125,000, and nearby towns and villages. The large loss of life (reportedly 5,000–20,000 casualties) and property was attributed to the collapse of buildings. In several places of the affected area, especially along Chlef river banks, great masses of sandy soils were ejected to the ground surface level. Belkhatir et al. [1] reported that a major damage to certain civil and hydraulic structures (earth dams, embankments, bridges, slopes and buildings) was caused by this earthquake.

Chlef city lies in a broad alluvial valley flanked to the north and south by ranges of hills that rise to a height of approximately 1,000 m. The valley is drained by the Chlef River. Although there was clear evidence of different types of soil failure, some of these failures occurred in a region where engineered structures existed; thus loss of life and property, because of soil failure, was important. Settlement of structures occurred, particularly in fill areas, and most backfills behind bridge abutments settled. Numerous slope failures were observed in the mountains, some involving the whole side of hills in the region attributable to fault movements. Some major slope failures were observed in the city of Chlef. Soil liquefaction occurred over widespread areas in the flood plain of the Chlef River, particularly in the region of Chlef and surrounding areas. Numerous sand boils were visible. Some of these were 4 m in diameter. Water spouting up to 2 m high was reported in many of the sand boil areas. Partially, and as a result of liquefaction subsidence, a large earthquake lake formed southeast of the canyon mouth where the Oued Fodda and Oued Chlef Rivers join and flow northwestward through the uplands on the upthrown block of the Oued Fodda fault.

Soil liquefaction is an important earthquake-induced hazard. During earthquake shaking or dynamic shearing, the undrained shear strength of saturated sandy soil mass decreases due to a rapid buildup of excess pore water pressure within a short time. When the excess pore pressure reaches the initial consolidation pressure level, the effective stress becomes zero, inducing a partial or a complete shear strength loss, called initial liquefaction. At the state of initial liquefaction, the soil mass behaves as a liquid, causing tremendous damage to soil foundations and earth structures. Sand boils, settlement or tilting of structures, failures of earth dams and slopes, lateral spreading of bridge foundations, landsliding and soil subsidence are some examples of liquefaction damage. Numerous researches have been reported on different factors influencing the soil liquefaction phenomenon such as the initial relative density, void ratio, sample preparation, sample size, grading characteristics, confinement, stress history, preshearing and loading conditions. However, many natural soils contain a significant amount of fines, and many unstable phenomena occur in soil layers with different amount of fines. Recent laboratory research works carried out by [1–11] have revealed that sand deposited with silt content can be much more liquefiable than clean sand. Also, strain properties and pore pressure generation in silty sand samples are quite different from those of clean sand. These new findings emphasize the important features of deposits with mixture of sand and silt. For example, the Nerlerk berm liquefaction slides in Canada in 1983 occurred in sands with a certain amount of silt contents according to [12]. Also, [13] reported that liquefaction occurred in silty sand and sandy silt in the 1988 Saguenay earthquake in Quebec. Yamamuro and Lade [6] summarized 14 cases of static liquefaction and 32 cases of liquefaction, resulting from earthquakes in silty soils all over the world. Some researchers have recently begun to study the monotonic and cyclic behavior of soils composed of sand–silt mixtures. However, published data related to the sand–silt mixture behavior are incomplete and require further investigation.

Liquefaction is a natural phenomenon which takes place in saturated loose and medium dense sands and silty sands. Laboratory studies related to liquefaction are often associated with the study of excess pore water pressure buildup of sand or silty sand. Liquefaction (or initial liquefaction) usually occurs if the excess pore water pressure becomes equal to the initial effective stress. In engineering practice, liquefaction analysis, using laboratory undrained shear strength data, involves the assessment of whether or not for a given loading condition; the excess pore water pressure parameter reaches the initial effective stress. The increase in excess pore water pressure below levels causing initial liquefaction may still be of a magnitude as to decrease the effective stress in the soil to levels consequential to the response of the soil deposit and to the stability and settlement of a structure founded on

Table 1 Index properties of tested materials

Material	F_c (%)	G_S	D_{10} (mm)	D_{50} (mm)	C_u	e_{min}	e_{max}	I_p (%)
Sand	0	2.680	0.22	0.68	3.36	0.535	0.876	–
Sand–silt mixtures	10	2.682	0.08	0.50	7.75	0.472	0.787	–
	20	2.684	0.038	0.43	15.26	0.431	0.729	–
	30	2.686	0.022	0.37	23.18	0.412	0.704	–
	40	2.688	0.015	0.29	27.33	0.478	0.796	–
	50	2.690	0.011	0.08	28.18	0.600	0.968	–
Silt	100	2.70	0.0017	0.039	27.65	0.72	1.137	5.0

these soil deposits. Thus, in practice, the determination of the appropriate excess pore water pressure buildup of sandy soils that are prone to liquefaction, to be used in the assessment of the liquefaction and post-liquefaction stability of earth structures, is becoming a major challenge [14].

This paper aimed to evaluate the effects of low plastic fines' fraction, gross and intergranular void ratios and relative density, on the generation of excess water pressure and undrained shear strength response of sand–silt mixtures. Thus, simple correlations for the prediction of peak shear strength and excess pore water pressure of sand–silt mixtures are suggested.

2 Laboratory Testing Program

2.1 Soil Index Properties

The soil samples used in this study were extracted from about 6.0 m below ground surface of the Chlef River banks, where liquefaction occurred during the 1980 El Asnam earthquake. Chlef sand has been used for all tests presented in this laboratory investigation. Individual sand particles are subrounded, and their predominant minerals are feldspar and quartz. The tests were conducted on the mixtures of Chlef sand and silt. Liquid limit and plastic limit of the silt are 27 and 22 % respectively. Chlef sand was mixed with 0–50 % silt to get different silt contents. The index properties of the sand and silt used in this laboratory work are presented in Table 1. The grain size distribution curves of the tested materials are shown in Fig. 1. The maximum void ratio (e_{max}) corresponding to the loosest state of the soil sample and minimum void ratio (e_{min}) corresponding to the densest state of the soil sample were determined according to ASTM D 4253 and ASTM D 4254 standards for 0–100 % range of fines' content (F_c). F_c is the ratio of the weight of silt to the total weight of the sand–silt mixture.

2.2 Sample Size

The dimensions of the samples were 70 mm in diameter and 70 mm in height ($H/D = 1$), in order to avoid the appearance

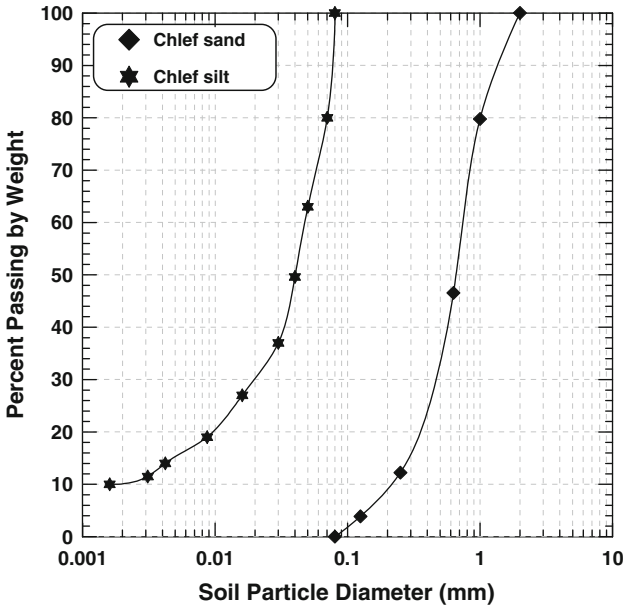

Fig. 1 Grain size distribution curves of tested materials

of shear banding (sliding surfaces) and buckling. To maintain a uniform density over the entire range of the sample height, the soil was prepared in seven layers and gently tamped in a symmetrical way on the sides of the sample mold. The lower layers were prepared at 1 % lesser density than the higher layers to maintain a uniform density through the entire range of the sample height. This method was first proposed by Ladd [15] and modified by Chan [16] and suggests a relative density difference of 1 % between two successive layers. The resulting height to diameter ratio of one was kept constant.

2.3 Sample Preparation

All samples were prepared by: first estimating the dry weights of sand and silt needed for a desired proportion into the loose and dense states ($D_r = 20$, 53 and 91 %) using undercompaction method of sample preparation which simulates a relatively homogeneous soil condition and is performed by compacting dry soil in layers to a selected percentage of the required dry unit weight of the specimen. The concept

of undercompaction is based on the fact that when successive layers of sand are placed without undercompaction, the compaction of each succeeding layer can further densify the sand below it. In order to avoid this difficulty, the lower layers were compacted to a lower density than desired for the final density. After the specimen has been formed, the specimen cap is placed and sealed with O-rings, and a partial vacuum of 15–25 kPa is applied to the specimen to reduce its probable disturbance.

2.4 Sample Saturation

Saturation was performed by purging the dry specimen with carbon dioxide for approximately 20 min. Deaired water was then introduced into the specimen from the bottom drain line. Water was allowed to flow through the specimen until an amount equal to the void volume of the specimen was collected in a beaker through specimen's upper drain line. A minimum Skempton coefficient value greater than 0.96 was obtained at a back pressure of 100 kPa.

2.5 Sample Consolidation

When samples were fully saturated, they were subjected to consolidation. During consolidation, the difference between all-around pressure and back pressure was set so that for each sample the effective consolidation pressure was fixed at 100 kPa.

2.6 Shear Loading

All undrained triaxial tests for this study were carried out at a constant strain rate of 0.167 % per minute, which was slow enough to allow pore pressure change to equalize throughout the sample, with the pore pressure measured at the base of sample. All tests were continued up to 24 % axial strain.

Laboratory research related to the fines' effect on the liquefaction resistance of silty sands has sometimes been based on the intergranular void ratio (sand skeleton void ratio) rather than the gross void ratio (sand–silt mixture void ratio). The concept of the intergranular void ratio calculates the void ratio while assuming that the volume occupied by the fines is part of the volume of voids. By neglecting the difference in the specific gravity of coarser and finer particles, an intergranular void ratio e_s was formulated as:

$$e_s = \frac{e + (G/G_f)(F_c/100)}{(1 - (G/G_f)(F_c/100))} \quad (1)$$

where G_f is the specific gravity of finer grain matrix, and G is the specific gravity of the sand–silt mixture. F_c is the fines' content, and e is the gross void ratio. Equation (1) gives the intergranular void ratio defined by Monkul and Yamamuro [17]. The concept of the intergranular void ratio suggests that

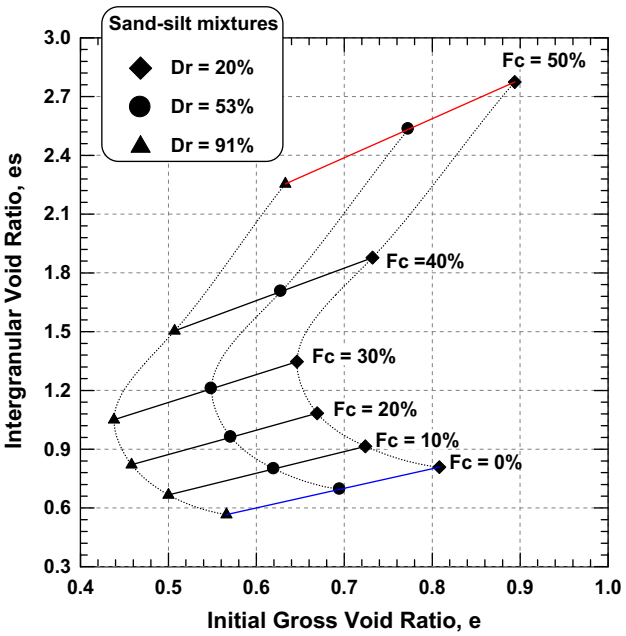

Fig. 2 Variation of the intergranular void ratio with the initial gross void ratio and fines' content ($\sigma_3' = 100$ kPa)

the fines fill the voids formed between the sand grains, and, thus, the behavior of sand with moderate amount of fines should be governed by the intergranular void ratio instead of the gross void ratio. However, when the intergranular void ratio exceeds the maximum gross void ratio of the clean sand, there are sufficient fines to prevent grain-to-grain contact of the sand particles. In this case, the fines constitute the dominant structure and carry the shear forces, while the coarse grains may act as reinforcing elements, as explained by Thevanayagam and Mohan [18].

Figure 2 shows the variation of the intergranular void ratio (the void ratio of the sand matrix after consolidation phase) versus the initial gross void ratio (the void ratio of the sand–silt mixture after consolidation phase) and the fines' content at relative densities of $D_r = 20$, 53 and 91 % respectively. As could be seen in this figure, the intergranular void ratio (e_s) increases hyperbolically with the decrease of the initial void ratio and with the increase of fines' content until the value of fines' content reaches 30 %. Beyond that, it increases linearly with the increase of the initial gross void ratio and fines' content. This shows that the gross void ratio does not represent the number of particles' contacts in silty sands. As the void ratio and the proportion of coarse to fine grains of soil changes, the nature of their microstructures also changes. Moreover, the slope of the intergranular void ratio line is more pronounced for higher fines' contents ($F_c = 30$, 40 and 50 %) in comparison with lower fines' contents ($F_c = 0$, 10 and 20 %) for the relative densities under consideration ($D_r = 20$, 53 and 91 %).

3 Monotonic Test Results

3.1 Undrained Compression Loading Tests

Figure 3 shows the results of the undrained monotonic compression triaxial tests carried out on different fines' contents ranging from 0 to 50 % at 100 kPa mean confining pressure, within the range of the three selected densities ($D_r = 20$, 53 and 91 %). We notice, in general, that the increase in the amount of low plastic fines leads to an increase of the pore water pressure (Fig. 3b). This increase results from the role of the low plastic fines ($I_p = 5$ %) in increasing the contraction phase of the sand–silt mixtures leading to a reduction of the confining effective pressure and, consequently, to a decrease of the peak resistance of the mixtures as illustrated in Fig. 3a. The stress path in the p', q plane shows clearly the role of the fines in the decrease of the average effective mean pressure and the decrease of the maximum deviatoric stress (Fig. 3c). These results are in good agreement with the observations of Shen et al. [19] and Troncoso and Verdugo [20].

Table 2 presents the summary of the undrained monotonic compression triaxial tests

3.2 Effect of the Initial Gross Void Ratio on Peak Strength

Figure 4 shows the peak shear strength versus the initial gross void ratio and initial relative density. It is clear from this figure that the peak shear strength decreases as the gross void ratio increases and initial relative density decreases for the entire range of 0–50 % fines' content under consideration. Therefore, the gross void ratio appears as a pertinent physical parameter characterizing the silty sand soil for a given fines' content. As the amount of low plastic fines increases, the peak shear strength decreases gradually. Lade and Yamamuro [3] explained this soil response in a way that low plastic fines makes sand–silt mixture structure more compressible and consequently the liquefaction resistance decreases. The following equation is suggested relating the peak shear strength to the gross void ratio for the different fines' contents under consideration:

$$\mathbf{log\left(q_{peak}\right) = B - A\,(e)} \tag{2}$$

Table 3 illustrates the coefficients A, B and the corresponding coefficient of determination (R^2) for the different fines' contents under study

3.3 Effect of Fines'Content on the Peak Strength

Figure 5 illustrates the peak shear strength versus fines' content. As it can be seen in this figure, the peak shear strength (q_{peak}) and the fines' content display a good linear relation. The peak shear strength decreases linearly with the increase of fines' content for the initial relative densities under consideration ($D_r = 20$, 53 and 91 %). The slope line of the peak shear strength of the dense material ($\alpha = 3.65$) is very pronounced compared to medium ($\alpha = 1.98$) and loose ($\alpha = 1.74$) material. The results of this research work are in good agreement with the findings of Lee and Fitton [21] and Singh [22]. This is also supported by the findings of Yilmaz et al. [23]; as the amount of fines content increases, the cyclic liquefaction resistance decreases gradually at a constant relative density of 60 %. In this laboratory investigation, for the range of 0–50 % fines' content in normally consolidated undrained triaxial compression tests, the following expression is suggested to evaluate the peak shear strength, which is a function of fines' content (F_c):

$$\mathbf{q_{peak} = B - A\,(F_c)} \tag{3}$$

Table 4 illustrates the coefficients A, B and the corresponding coefficient of determination (R^2) for the different initial relative densities under consideration.

3.4 Effect of the Initial Intergranular Void Ratio on Peak Strength

Figure 6 shows the peak shear strength versus the initial intergranular void ratio. It is clear from this figure that the peak shear strength decreases with the increase of the intergranular void ratio for the different fines' contents under study. However, for a given fines' content, the peak shear strength decreases with the increase of the intergranular void ratio and decrease of the initial relative density. It seems that the variation of the peak shear strength (q_{peak}) due to the amount of fines is related to the intergranular void ratio in the range 0–50 % fines' content. In this case, the behavior of sand–silt mixture samples is influenced by the contacts of coarser grains, which is solely quantified by the intergranular void ratio. By increasing the fines' content in the range of 0–50 %, the contacts between sand grains decrease and consequently the intergranular void ratio increases while the peak shear strength (q_{peak}) decreases. Moreover, the slope of the peak shear strength line is very pronounced for smaller fines' contents ($\alpha = 550.77$) in comparison with higher fines' contents ($\alpha = 70.20$). This behavior can be explained by the fact that the increase of low plastic fines' amount makes the structure of the sand–silt mixtures more compressible. For a given fines' content, the peak shear strength correlates very well with the intergranular void ratio. The following expression is suggested to evaluate the peak shear strength, which is a function of intergranular void ratio (e_s) for given fines' contents under consideration:

$$\mathbf{q_{peak} = B - A\,(e_s)} \tag{4}$$

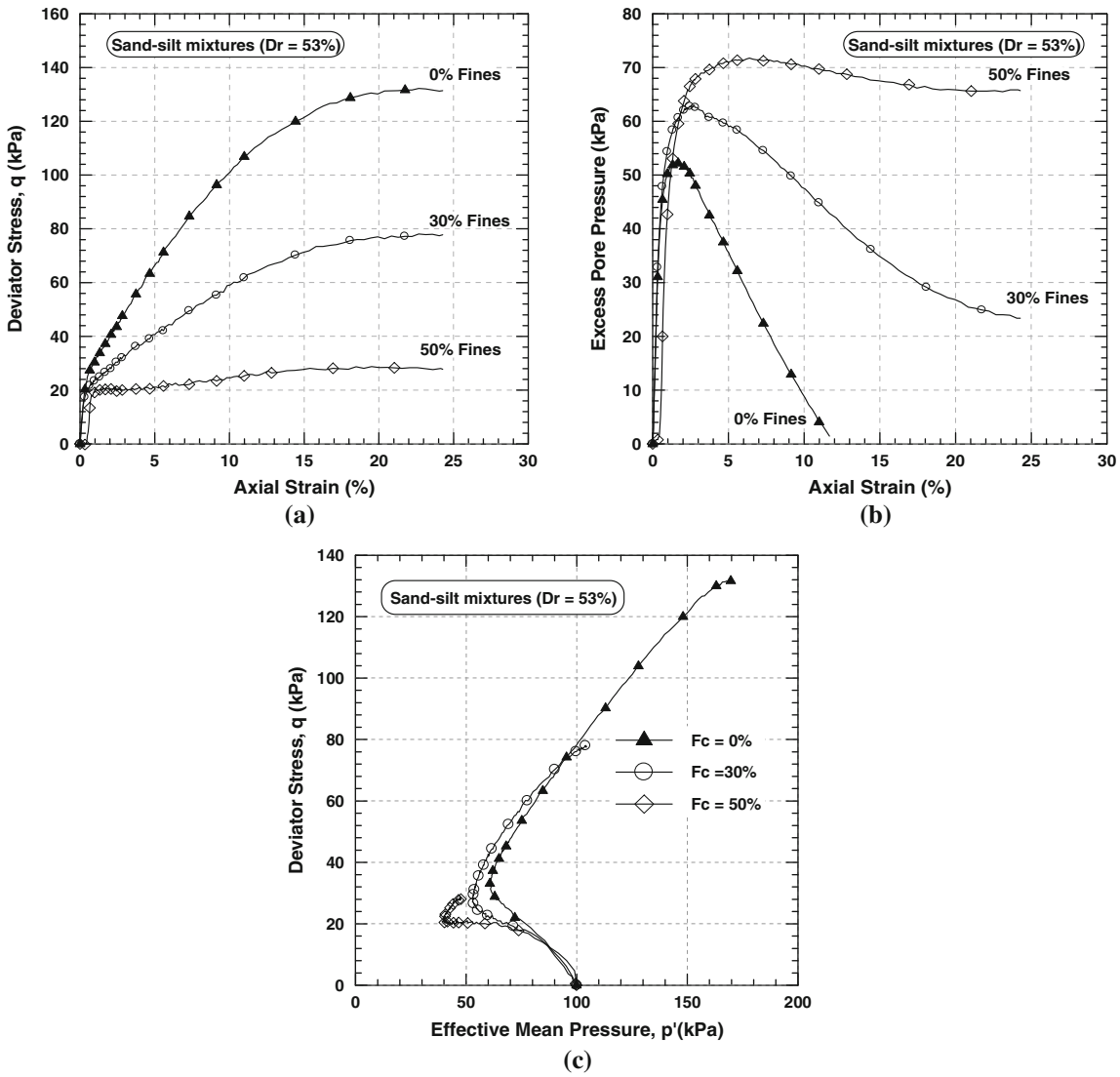

Fig. 3 Undrained monotonic response of the sand–silt mixtures at $F_c = 0$, 30 and 50 % ($\sigma_3' = 100$ kPa, $D_r = 53$ %)

Table 5 illustrates the coefficients A, B and the corresponding coefficient of determination (R^2) for the selected fines' contents under consideration.

3.5 Effect of Initial Relative Density on Peak Strength

Figure 7 shows the variation of peak shear strength (q_{peak}) versus initial relative density (D_r) at various fines' contents. It is clear from this figure that the peak shear strength increases with the increase of initial relative density for all fines' contests. Thevanayagam et al. [4] and Sitharam et al. [24] have reported similar behavior of increasing undrained shear strength with increasing relative density. The present laboratory study focuses on the effect of fines' content and other parameters on the undrained shear strength of sand–silt mixtures at three initial relative densities ($D_r = 20$, 53 and 91 %). It can be noticed from the results of this study that there is a significant decrease in the peak shear strength with the increase in fines' content for the three initial relative densities selected in this investigation. Moreover, the slope of the peak strength line is very pronounced for smaller fines' contents ($F_c = 0$, 10 and 20 %) compared with higher fines' contents ($F_c = 30$, 40 and 50 %). The outcome of the present study is in good agreement with the experimental work reported by Ishihara [25] on Tia Juana silty sand, by Baziar and Dobry [26] on silty sands retrieved from the Lower San Fernando Dam and by Naeini and Baziar [9] on Adebil sand with different fines' contents. The following expression is suggested to evaluate the peak shear strength, which is a function of initial relative density (D_r) for the fines' contents under study:

$$\mathbf{q_{peak}} = \mathbf{B} + \mathbf{A}\,(\mathbf{D_r}) \tag{5}$$

Table 2 Summary of monotonic compression triaxial test results

Test no.	Material	F_C (%)	D_r (%)	γ_d (g/cm^3)	e	e_s	q_{peak} (kPa)	Δu (kPa)
1	Sand	0	20	1.48	0.808	0.808	97.50	62.0
2			53	1.58	0.695	0.695	132.23	52.19
3			91	1.71	0.566	0.566	229.60	48.20
4	Silty sand	10	20	1.56	0.724	0.914	84.50	65.20
5			53	1.65	0.620	0.799	114.20	55.59
6			91	1.79	0.500	0.666	191.70	50.70
7		20	20	1.61	0.669	1.083	57.20	70.60
8			53	1.71	0.571	0.961	91.57	60.78
9			91	1.84	0.458	0.820	168.30	53.20
10		30	20	1.63	0.646	1.346	36.80	76.00
11			53	1.73	0.549	1.208	78.08	63.00
12			91	1.87	0.438	1.050	108.60	56.20
13		40	20	1.55	0.732	1.878	20.80	78.30
14			53	1.65	0.628	1.705	61.15	68.13
15			91	1.78	0.507	1.504	77.70	60.7
16		50	20	1.42	0.894	2.774	17.90	82.70
17			53	1.52	0.773	2.533	28.42	71.76
18			91	1.65	0.633	2.254	54.10	66.50

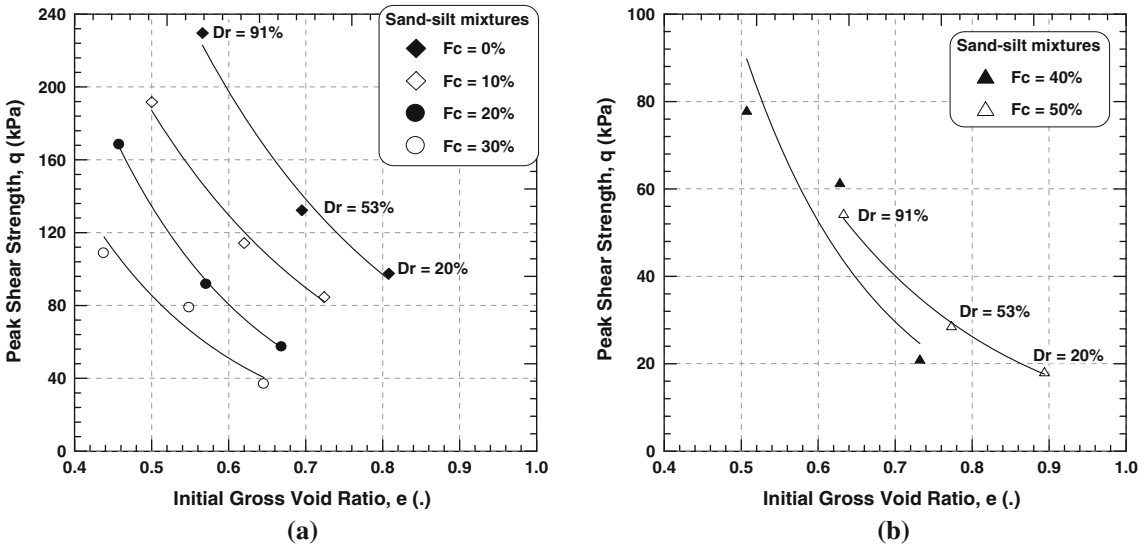

Fig. 4 Variation of the peak strength with the initial gross void ratio, fines' content and relative density ($\sigma_3' = 100$ kPa)

Table 6 illustrates the coefficients A, B and the corresponding coefficient of determination (R^2) for the selected fines' contents under study.

3.6 Effect of Initial Gross Void Ratio on Pore Pressure

Figure 8 shows the excess pore pressure versus the initial gross void ratio at different fines' content. It is clear from Fig. 8a that the excess pore pressure increases as the initial gross void ratio decreases, and fines' content increases for the loose, medium and dense state ($D_r = 20$, 53 and 91 %) up to 30 % fines' content. Beyond 30 % of fines' content, the excess pore pressure continues to increase with increasing gross void ratio and fines' content for the three relative densities under consideration ($D_r = 20$, 53 and 91 %). However, for a given fines' content, the excess pore pressure decreases linearly with the decrease of the initial gross void ratio and with the increase of the initial relative density (Fig. 8b). Moreover,

Table 3 Coefficients A, B and R^2 for Eq. (2)

F_c (%)	A	B	R^2
0	3.56	7.42	0.98
10	3.67	7.07	0.99
20	5.12	7.46	0.99
30	5.15	7.02	0.93
40	5.75	7.41	0.85
50	4.25	6.66	0.99

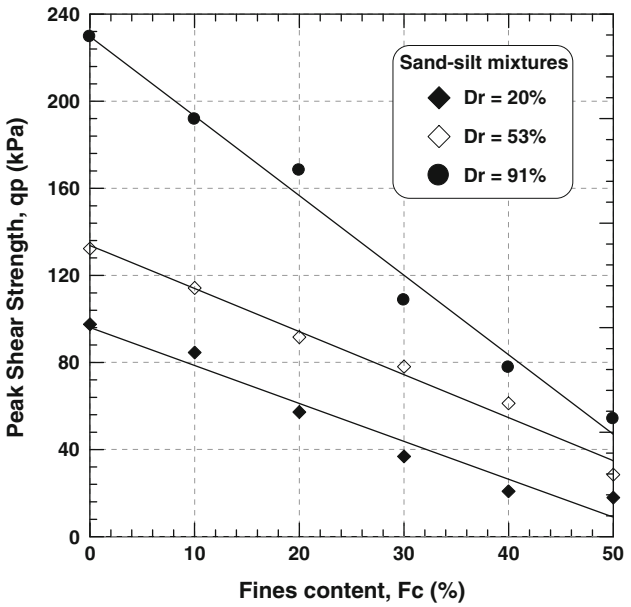

Fig. 5 Peak shear strength versus fines' content at various initial relative densities ($\sigma_3' = 100$ kPa)

Table 4 Coefficients A, B and R^2 for Eq. (3)

D_r (%)	A	B	R^2
20	1.74	95.98	0.96
53	1.98	133.68	0.98
91	3.65	229.71	0.98

the slope of the excess pore pressure line reaches a maximum value ($\alpha = 94.38$) at a fines' content of 30 %. The following expression is suggested to evaluate the excess pore water pressure versus the initial gross void ratio (e):

$$\mathbf{\Delta u = B + A\,(e)} \tag{6}$$

Table 7 illustrates the coefficients A, B and the corresponding coefficient of determination (R^2) for the selected fines' contents.

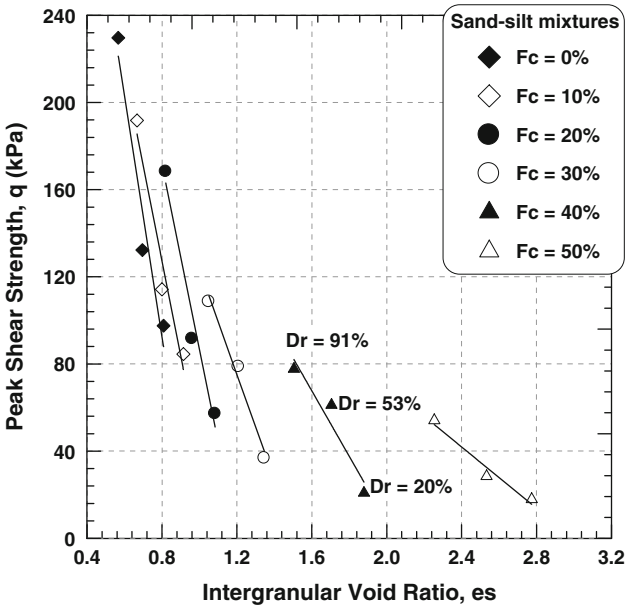

Fig. 6 Variation of the peak shear strength with initial intergranular void ratio and fines' content ($\sigma_3' = 100$ kPa)

Table 5 Coefficients A, B and R^2 for Eq. (4)

F_c (%)	A	B	R^2
0	550.77	532.96	0.95
10	436.16	476.00	0.96
20	425.57	511.97	0.97
30	241.27	364.58	0.98
40	150.27	308.03	0.92
50	70.20	210.40	0.96

3.7 Effect of Fines Content on Pore Pressure

Figure 9 shows the variation of the excess pore pressure versus fines' content. As it can be seen from this figure, the excess pore pressure of the sand–silt mixtures (Δu) increases linearly with the increase of fines' content for the three initial relative densities ($D_r = 20$, 53 and 91 %). We notice that the excess pore pressure slope line remains nearly the same for the range of fines' contents and initial relative densities under consideration. For a given fines' content, the excess pore pressure increases with the decrease of the initial relative density. There is a relatively high degree of correlation between the excess pore pressure (Δu) and the fines' content (F_c) for the initial relative densities under study. In this laboratory investigation, and for the range of 0–50 % fines' content in normally consolidated undrained triaxial compression tests, the following expression is suggested to evaluate the excess pore pressure which is a function of fines' content (F_c):

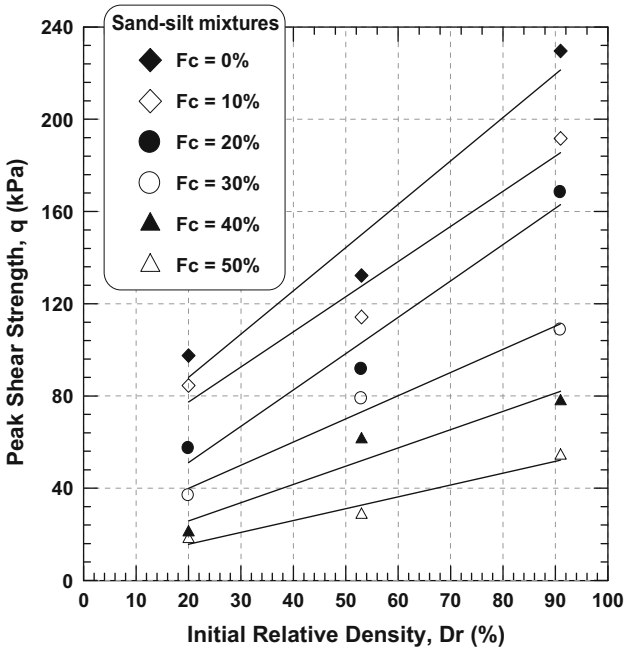

Fig. 7 Peak strength versus initial relative density at various fines' contents ($\sigma_3' = 100$ kPa)

Table 6 Coefficients A, B and R^2 for Eq. (5)

F_c (%)	A	B	R^2
0	1.88	50.43	0.95
10	1.52	46.86	0.96
20	1.57	19.52	0.97
30	1.01	19.76	0.98
40	0.79	9.91	0.92
50	0.51	5.37	0.96

$$\mathbf{\Delta u = B + A\,(F_c)} \tag{7}$$

Table 8 illustrates the coefficients A, B and the corresponding coefficient of determination (R^2) for the selected initial relative densities under consideration.

3.8 Effect of the Intergranular Void Ratio on Excess Pore Pressure

Figure 10 presents the variation of the excess pore pressure versus the intergranular void ratio and initial relative density. It is clear from this figure that the excess pore water pressure increases linearly with the increase of the intergranular void ratio and the decrease of the initial relative density for the range of fines' content under consideration. The excess pore water pressure slope line decreases with the increase of intergranular void ratio and initial relative density. Moreover, the slope of the excess pore pressure line is higher for smaller fines' contents ($F_c = 0$, 10, 20 and 30 %) in comparison with higher fines' contents ($F_c = 40$ and 50 %). The following expression is suggested to relate the excess pore water pressure to the intergranular void ratio:

$$\mathbf{\Delta u = B + A\,(e_s)} \tag{8}$$

Table 9 illustrates the coefficients A, B and the corresponding coefficient of determination (R^2) for the selected fines' contents

3.9 Effect of Relative Density on Excess Pore Water Pressure

Figure 11 shows the variation of the excess pore pressure (Δu) versus initial relative density (D_r) at fines' content ranging from 0 to 50 %. It is clear from this figure that an increase in the initial relative density results in a decrease in the excess pore pressure at a given fines' content. However, the excess pore water pressure increases with the increase of fines' content at a selected initial relative density. For a selected fines' content, the excess pore water pressure correlates very well with the initial relative density for the range of fines' content under consideration. The following expression is suggested to evaluate the excess pore water pressure, which is a function of initial relative density (D_r):

$$\mathbf{\Delta u = B + A\,(D_r)} \tag{9}$$

Table 10 illustrates the coefficients A, B and the corresponding coefficient of determination (R^2) for the selected fines' contents

3.10 Relationship Between Pore Pressure and Undrained Peak Shear Strength

Figure 12 shows the variation of the peak shear strength (q_{peak}) with the excess pore pressure (Δu) at various fines' contents. It is clear from this figure that the peak shear strength decreases with the increase of the excess pore water pressure. There is a relatively high degree of correlation between the peak shear strength (q_{peak}) and the excess pore pressure (Δu) for the three investigated relative density tests ($R^2 = 0.95$ for $D_r = 20$ %, $R^2 = 0.86$ for $D_r = 53$ % and $R^2 = 0.99$ for $D_r = 91$ %). The following expression is suggested to predict the peak shear strength as a function of the excess pore water pressure for the range of 0–50 % fines' content:

$$\mathbf{\log\left(q_{peak}\right) = B - A\,\log(\Delta u)} \tag{10}$$

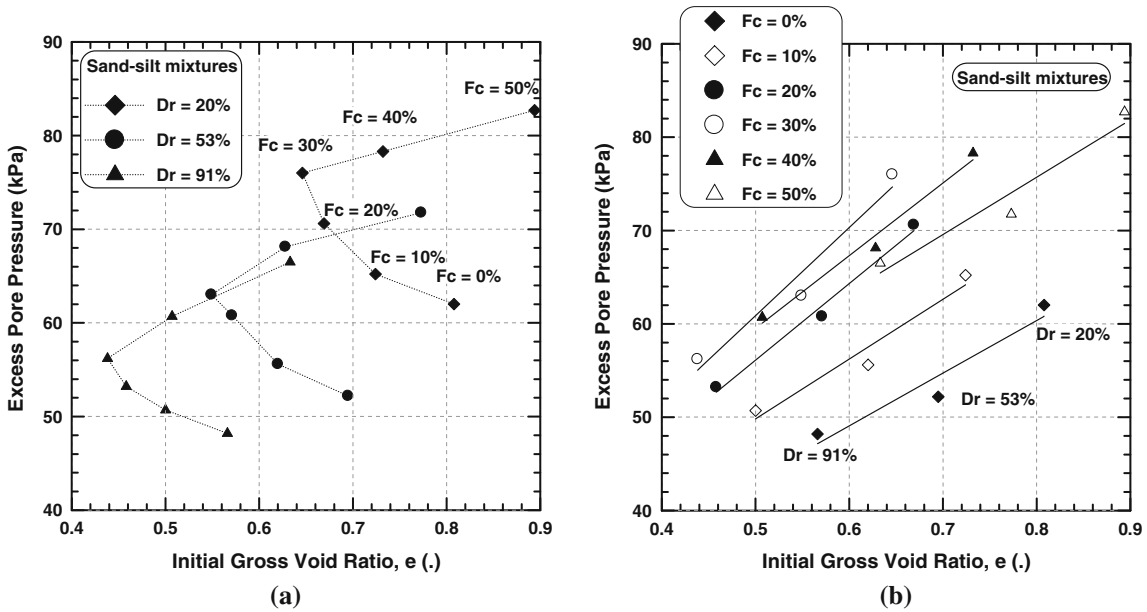

Fig. 8 Excess pore pressure versus initial gross void ratio at various fines' contents ($\sigma_3' = 100\,\text{kPa}$)

Table 7 Coefficients A, B and R^2 for Eq. (6)

F_c (%)	A	B	R^2
0	56.41	15.22	0.93
10	64.12	17.75	0.95
20	82.07	15.07	0.99
30	94.38	13.69	0.95
40	77.77	20.65	0.98
50	61.43	26.55	0.94

Table 11 illustrates the coefficients A, B and the corresponding coefficient of determination (R^2) for the selected initial relative densities under consideration.

3.11 Comparison with Published Literature

To compare the present laboratory investigation results with other published data related to the influence of low plastic fines on the liquefaction resistance of sand–silt mixtures, the initial conditions used as a basis for comparison purposes must be taken into account.

Different published findings revealed that the effect of low plastic fines on the liquefaction resistance of sand–silt mixtures can be drawn depending on the type of approach used (initial relative density, global void ratio, intergranular void ratio or interfine void ratio). Xenaki and Athanasopoulos [27] reported that the liquefaction resistance of sand–silt mixtures may either decrease or increase with increasing values of fines content, when compared at the same global void ratio, indicating the existence of a threshold value of fines' content ($F_{\text{cth}} = 44\,\%$). Xenaki and Athanasopoulos [27] noted that the threshold value of fines' content, F_{cth}, is not unique but it may depend on the characteristics of the coarse and fine grains, as well as on the characteristics of the global void ratio, e, of the sand–silt mixture. Troncoso [28] found that the liquefaction resistance of sand–silt mixtures decreases with increasing the fines' content (up to 30 %)

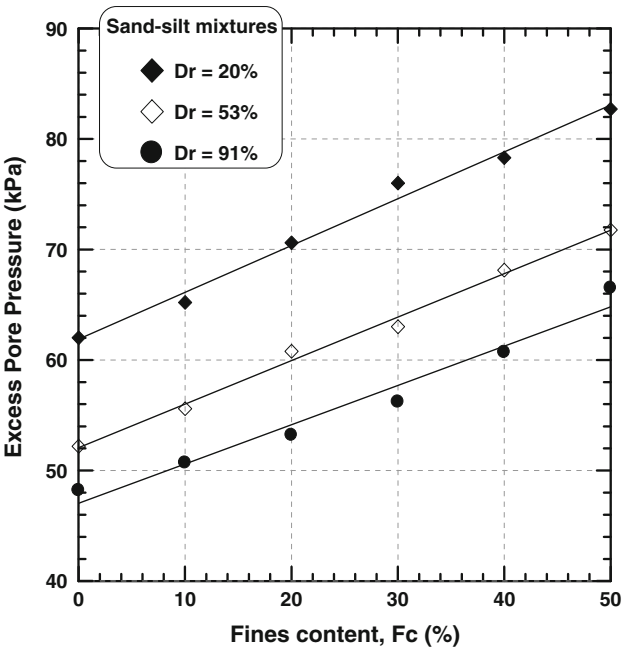

Fig. 9 Excess pore pressure versus fines' content at various relative densities ($\sigma_3' = 100\,\text{kPa}$)

Table 8 Coefficients A, B and R^2 for Eq. (7)

F_c (%)	A	B	R^2
20	0.42	61.88	0.99
53	0.39	52.07	0.99
91	0.36	47.02	0.97

when the global void ratio approach is used. The experimental results of the present study are in perfect agreement with the sand–silt mixture response reported by Troncoso [28]. On the other hand, [29] and [30] reported that beyond critical value of fines' content, the liquefaction resistance increases with the increase of the fines' content. The data published by Polito [31] revealed the existence of threshold value of fines' content ranging from 25 to 45 %. Regarding the nature of fines, [29] reported that the effect of plasticity of fines on the liquefaction resistance of sand–fines mixtures is less marked compared to the corresponding effect of fines' content. It is worth to mention in this context that [32] showed that the fines' content alone is not a pertinent parameter to be correlated with the liquefaction resistance. The results of this investigation indicated that the sand–fines mixture cyclic resistance is related to the fines' content and plasticity index of the fines.

Finally, it should be mentioned that [33] indicated that, although global void ratio constitutes a better parameter than relative density to explain the effect of fines on the sand–fines mixture liquefaction resistance, the interpretation in terms of global void ratio may not be appropriate. Therefore, [18] used the concept of the intergranular void ratio, e_s, to characterize the silty soils reported in their study. They proposed to view the matrix of sand with fines as a combination of two sub-matrices: coarser grain matrix and a finer grain matrix. Consequently, they suggested that for fines' content F_c (i.e., expressed as a percentage of the total weight of the soil specimen) below a limit in the range of 20–30 %, the contribution of fines in the force chain is minimal. The significance of e_s has been recently recognized, and several studies have shown that the liquefaction resistance of sand–fines mixtures is closely related to both fines' content and intergranular void ratio. In agreement with the results of the current study, the results reported by Abedi and Yasrobi [34] indicated that when compared at the same initial relative density, the liquefaction resistance of sand–fines decreases with the increase of fines' content.

4 Conclusion

A comprehensive laboratory investigation was undertaken to study the influence of fines' content, in terms of gross and intergranular void ratios and initial relative density, on excess pore pressure generation and undrained shear strength characteristics, through a series of undrained monotonic triaxial tests that were carried out on sand–silt mixtures collected from liquefied sites at Chlef River, Algeria. In light of the experimental evidence, the following conclusions can be drawn:

1. The analysis of the obtained data revealed that the presence of low plastic fines' fraction has significant influence on the generation of the excess pore water pressure. Sand–silt samples with 50 % fines' content exhibited an average of 35 % excess pore water pressure increase, when compared to sand without fines for the initial relative densities under consideration (D_r = 20, 53 and 91 %). This is supported by the findings of [22] where cyclic excess pore pressure of sand–silt mixtures reconstituted with 10, 20 and 30 % fines' content is somewhat higher compared to clean sand at an initial relative density of 50 %.

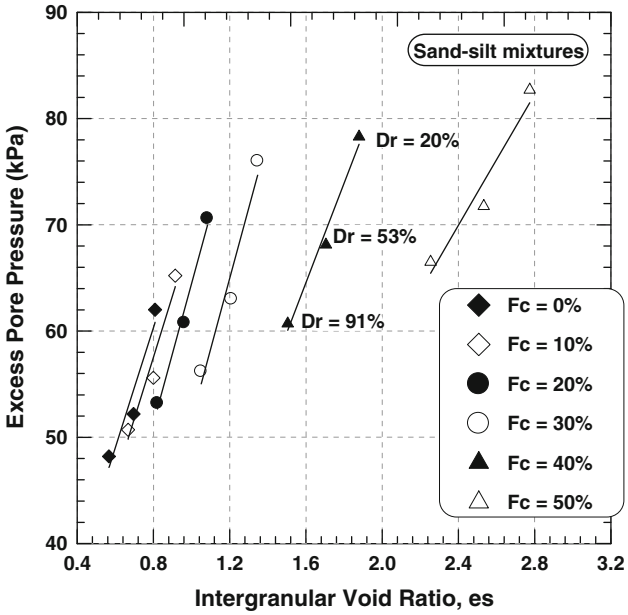

Fig. 10 Excess pore pressure versus intergranular void ratio at various fines' contents ($\sigma_3' = 100\,kPa$)

Table 9 Coefficients A, B and R^2 for Eq. (8)

F_c (%)	A	B	R^2
0	56.41	15.22	0.93
10	57.91	11.24	0.95
20	65.84	−1.33	0.99
30	66.32	−14.60	0.95
40	46.79	−10.29	0.98
50	30.83	−4.06	0.94

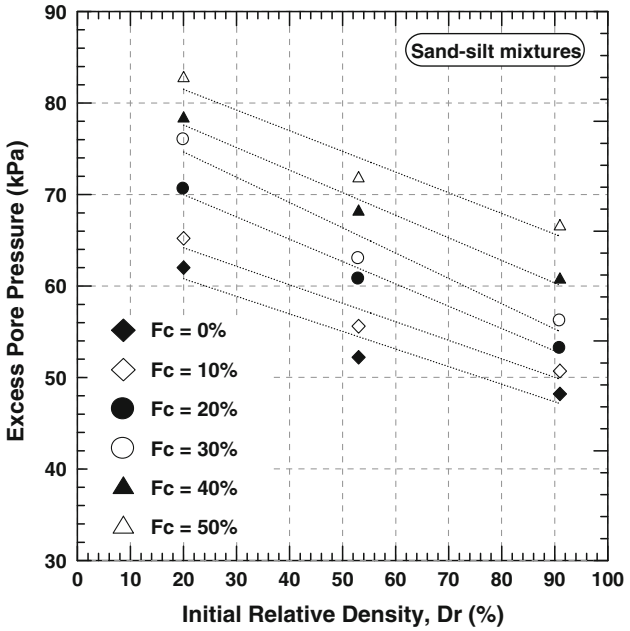

Fig. 11 Excess pore pressure versus initial relative density at various fines' contents ($\sigma_3' = 100\,\text{kPa}$)

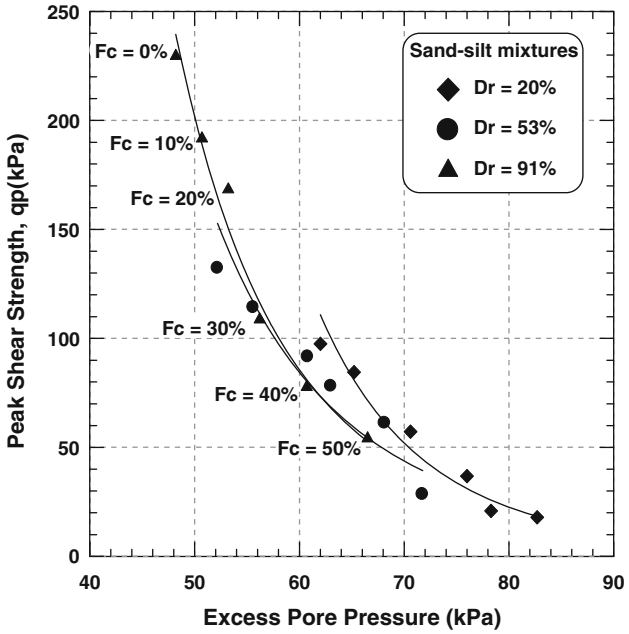

Fig. 12 Peak shear strength versus excess pore pressure at various fines' contents ($\sigma_3' = 100\,\text{kPa}$)

Table 10 Coefficients A, B and R^2 for Eq. (9)

F_c (%)	A	B	R^2
0	−0.19	64.63	0.92
10	−0.20	68.22	0.95
20	−0.24	74.86	0.99
30	−0.28	80.17	0.95
40	−0.25	82.52	0.98
50	+0.23	86.00	0.94

Table 11 Coefficients A, B and R^2 for Eq. (10)

D_r (%)	A	B	R^2
20	6.25	30.50	0.95
53	4.26	21.89	0.86
91	4.70	23.70	0.99

2. The excess pore water pressure decreases linearly with the decrease of the initial gross void ratio and with the increase of the initial relative density for a given fines' content. Moreover, the slope of the excess pore pressure line reaches a maximum value at a fines' content of 30 % and then decreases with an increase or decrease of fines' content.
3. The excess pore water pressure of the sand–silt mixtures (Δu) increases linearly with the increase of fines' content for the three initial relative densities ($D_r = 20$, 53 and 91 %). We notice that the excess pore pressure slope line increases with the increase of the initial relative density for the range of the fines' contents tested. For a given fines' content, the excess pore pressure increases with the decrease of the initial relative density.
4. The excess pore water pressure increases linearly with the increase of the intergranular void ratio and with the decrease of the initial relative density, for a given fines' content. The excess pore water pressure slope line decreases with the increase of intergranular void ratio and initial relative density. Moreover, the slope of the excess pore pressure line is higher for smaller fines' contents ($F_c = 0$, 10, 20 and 30 %) in comparison with higher fines' contents ($F_c = 40$ and 50 %).
5. For a given fines' content, the excess pore water pressure correlates very well with the initial relative density for the range of fines' content under consideration. An increase in the initial relative density results in a decrease in the excess pore pressure at a given fines' content. However, the excess pore water pressure increases with the increase of fines' content at a given relative density.
6. The peak shear strength decreases with the increase of the excess pore water pressure. There is a relatively high degree of correlation between the peak shear strength (q_{peak}) and the excess pore pressure (Δu) for the three investigated relative density tests ($R^2 = 0.95$ for $D_r = 20$ %, $R^2 = 0.86$ for $D_r = 53$ % and $R^2 = 0.99$ for $D_r = 91$ %).

Acknowledgments The authors would like to thank the reviewers for their constructive and valuable comments that have positively impacted

and brought it real close to the ultimate goal. All tests were carried out in the Laboratory of Material Sciences & Environment at Hassiba Benbouali of Chlef (Algeria) and Laboratory of Foundation Engineering, Soil & Rock Mechanics at Ruhr University of Bochum (Germany). The authors acknowledge the technicians who contributed in this experimental program.

References

1. Belkhatir, M.; Arab, A.; Della, N.; Missoum, H.; Schanz, T.: Influence of inter-granular void ratio on monotonic and cyclic undrained shear response of sandy soils. C. R. Mecanique **338**, 290–303 (2010)
2. Zlatovic, S.; Ishihara, K.: On the influence of non-plastic fines on residual strength. In: Proceedings of the First International Conference on Earthquake Geotechnical Engineering. Tokyo, 14–16 (1995)
3. Lade, P.V.; Yamamuro, J.A.: Effects of non-plastic fines on static liquefaction of sands. Can. Geotech. J. **34**, 918–928 (1997)
4. Thevanayagam, S.; Ravishankar, K.; Mohan, S.: Effects of fines on monotonic undrained shear strength of sandy soils. ASTM Geotech. Test. J. **20**(1), 394–406 (1997)
5. Thevanayagam, S.: Effect of fines and confining stress on undrained shear strength of silty sands. J. Geotech. Geoenviron. Eng. Div. ASCE **124**(6), 479–491 (1998)
6. Yamamuro, J.A.; Lade, P.V.: Steady-state concepts and static liquefaction of silty sands. J. Geotech. Geoenviron. Eng. ASCE **124**(9), 868–877 (1998)
7. Amini, F.; Qi, G.Z.: Liquefaction testing of stratified silty sands. J. Geotech. Geoenviron. Eng. Proc. ASCE **126**(3), 208–217 (2000)
8. Naeini, S.A.: The influence of silt presence and sample preparation on liquefaction potential of silty sands. PhD Dissertation, Tehran, Iran: Iran University of Science and Technology (2001)
9. Naeini, S.A.; Baziar, M.H.: Effect of fines content on steady-state strength of mixed and layered samples of a sand. Soil Dyn. Earthq. Eng. **24**, 181–187 (2004)
10. Sharafi, H.; Baziar, M.H.: A laboratory study on the liquefaction resistance of Firouzkooh silty sands using hollow torsional system. EJGE **15**, 973–982 (2010)
11. Belkhatir, M.; Arab, A.; Della, N.; Missoum, H.; Schanz, T.: Liquefaction resistance of Chlef river silty sand : effect of low plastic fines and other parameters. Acta Polytech. Hung. **7**(2), 119–137 (2010)
12. Sladen, J.A.; D'Hollonder, R.D.; Krahn, J.; Mitchell, D.E.: Back analysis of the Nerlek berm liquefaction slides. Can. Geotech. J. **22**, 579–588 (1985)
13. Troncoso, J.H.: Evaluation of seismic behaviour of hydraulic structures. Geotechnical special publication. no. 21, pp. 475–491 (1988)
14. Belkhatir, M.; Arab, A.; Schanz, T.; Missoum, H.; Della, N.: Laboratory study on the liquefaction resistance of sand–silt mixtures: effect of grading characteristics. Granul. Matt. **13**(5), 599–609 (2011)
15. Ladd, R.S.: Preparing test specimen using under compaction. Geotech. Test. J. GTJODJ **1**, 16–23 (1978)
16. Chan C.K.: Instruction manual, CKC E/P cyclic loading triaxial system user's manual. Soil Engineering Equipment Company, San Francisco (1985)
17. Monkul, M.M.; Yamamuro, J.A.: Influence of silt size and content on liquefaction behaviour of sands. Can. Geotech. J. **48**, 931–942 (2011)
18. Thevanayagam, S.; Mohan, S.: Inter-granular state variables and stress-strain behaviour of silty sands. Geotechnique **50**(1), 1–23 (2000)
19. Shen, C.K.; Vrymoed, J.L.; Uyeno, C.K.: The effects of fines on liquefaction of sands. In: Proceedings of the 9th International Conference Soil Mechanics and Foundation Engineering, Tokyo, vol. 2, pp. 381–385 (1977)
20. Troncoso, J.H.; Verdugo, R.: Silt content and dynamic behaviour of tailing sands. In: Proceedingsof the 12th International Conference on Soil Mechanics and Foundation Engineering, San Francisco, pp. 1311–1314 (1985)
21. Lee, K.L.; Fitton, J.A.: Factors affecting the cyclic strength of soil. Vib. Effects Earthq. Soils Found. ASTM STP Am. Soc. Test. Mater. **450**, 71–95 (1968)
22. Yilmaz, Y.; Mollamahmutoglu, M.; Ozaydin, V.; Kayabali, K.: Experimental investigation of the effect of grading characteristics on the liquefaction resistance of various graded sands. Eng. Geol. J. **100**, 91–100 (2008)
23. Yilmaz, Y.; Mollamahmutoglu, M.; Ozaydin, V.; Kayabali, K.: Experimental investigation of the effect of grading characteristics on the liquefaction resistance of various graded sands. Eng. Geol. J. **100**, 91–100 (2008)
24. Sitharam, T.G.; Govinda Raju, L.; Srinivasa Murthy, B.R.: Cyclic and monotonic undrained shear response of silty sand from Bhuj region in India. ISET J. Earthq. Technol. Paper No 450 **41**(2–4), 249–260 (2004)
25. Ishihara, K.: Liquefaction and flow failure during earthquakes. Geotechnique **43**(3), 351–415 (1993)
26. Baziar, M.H.; Dobry, R.: Residual strength and large-deformation potential of loose silty sands. J. Geotech. Eng. ASCE **121**, 896–906 (1995)
27. Xenaki, V.C.; Athanasopoulos, G.A.: Liquefaction resistance of sand–silt mixtures: an experimental investigation of the effect of fines. Soil Dyn. Earthq. Eng. **23**, 183–194 (2003)
28. Troncoso, J.H.: Failure risks of abandoned tailing dams. In: Proceedings of the International Symposium on Safety and Rehabilitation of Tailing Dams, International Commission on Large Dams, Paris, pp. 82–89 (1990)
29. Koester, J.P.: The influence of fines types and content on cyclic strength. In: Prakash, S.; Dakoulas, P. (eds.) Ground Failures Under Seismic Conditions. ASCE Geotechnical Special Publication, vol. 44, pp. 17–33 (1994)
30. Polito, C.P.; Martin, J.R. II.: Effects of nonplastic fines on the liquefaction resistance of sands. J. Geotech. Geoenviron. Eng. **127**((5), 408–415 (2001)
31. Polito, C.P.: The effects of non-plastic and plastic fines on the liquefaction of sandy soils. PhD Thesis, Virginia Polytechnic Institute and State University, Blacksburg (1999)
32. Ishihara, K.; Troncoso, J.; Kawase, Y.; Takahashi, Y.: Cyclic strength characteristics of tailings materials. Soils Found. **20**(4), 127–142 (1980)
33. Singh, S.: Liquefaction characteristics of silts: Geotech. Geol. Eng. **14** (1), 1–19 (1996)
34. Abedi, M.; Yasrobi, S.S.: Effects of plastic fines on the instability of sand. Soil Dyn. Earthq. Eng. **30**, 61–67 (2010)